One-Dimensional Leaky-Wave Antennas with Narrow Beam and Low Sidelobes

Gerard Zamora, *Member, IEEE* and Jordi Bonache, *Member, IEEE*

***Abstract*—A new technique for designing one-dimensional (1D) leaky-wave antennas (LWAs) with narrow main beam and low sidelobe level (SLL) is proposed in this paper. The presented method consists in connecting two open waveguiding structures designed to propagate a leaky wave with opposite phase velocities. The feed is positioned at the intersection plane where the two branches are connected and is chosen to excite the propagative mode guaranteeing continuity of phase at said intersection plane. Thus, a unidirectional leaky wave will travel from one end of the structure to the other with a double exponential amplitude distribution. The provided analysis shows that, compared to conventional (single-sided) LWAs of the same length, and compared to bidirectional LWAs of the same length operating at an off-broadside angle, the beamwidth can be considerably reduced and the sidelobe level (SLL) can be concurrently reduced to a significant degree. Additionally, the directivity may also be increased. To verify the presented technique and theory, a demonstrating prototype using split-ring-resonators (SRRs) and microstrip technology is designed, fabricated, and measured. A single-sided 1D LWA is also fabricated and measured for comparison purposes. The experimental results confirm the proposed approach.**

***Index Terms*—Leaky-wave antennas (LWAs), metamaterials, composite right/left-handed (CRLH), Split Ring Resonator (SRR), microstrip.**

I. Introduction

ONE-dimensional (1D) leaky-wave antennas (LWAs) are a particular class of LWAs whose structure supports a fast wave traveling in a fixed direction. They have received much attention in the last decades, mainly due to the advent of metamaterial transmission lines [1], [2]. Specifically, the interest in 1D planar LWAs has recently increased due to their structural simplicity, low profile, integration with other planar components, and cost effectiveness [3]-[6].

There are three different categories of LWAs: uniform, quasi-uniform and periodic. In uniform LWAs the guiding structure have a constant geometry along the length and uses the dominant or a higher-order fast-wave mode. Conversely, periodic LWAs consist of a uniform slow-wave structure which has been periodically modulated. The periodic modulation produces an infinite number of space harmonics (Floquet waves), some of which may be fast, hence providing leaky-wave radiation. Finally, quasi-uniform structures are also characterized by a periodic modulation of their geometry. In this case, however, the period is small enough (much smaller than the guided wavelength of the traveling wave) such that radiation comes from the fundamental space harmonic, which is the only significant one [6].

Leaky waves are characterized by a complex wavenumber, which determines the main features of the radiation pattern: the angle of the main beam, beamwidth, and sidelobe level. The real part β and the imaginary part α of the complex wavenumber correspond to the phase constant and the leakage rate (or attenuation constant, in the dissipative scenario) of the leaky wave, respectively. Since radiation losses reduce the amplitude as the wave travels through the structure, the modes inside the structure will show an exponentially-decaying-amplitude profile which implies poor sidelobe features [7]. For this reason, the standard technique to reduce the sidelobe level (SLL) is focused on the control of the near-field illumination, rather than in the control of the current distribution of the propagating modes present in the structure. Typically, the cross section of the LWA is tapered to achieve a symmetrical near-field illumination pattern that provides a given SLL, such as uniform, cosine or Taylor distribution (e.g., by means of slots of varying width in one of the walls of a waveguide) [4], [8]-[13]. The most difficult part of this technique lies on the fact that half part of the radiator must show an increasing profile of the near-field illumination, while the mode travelling inside the structure shows a decreasing profile.

The amplitude taper of the aperture illumination can be avoided by considering 1D LWAs that support bidirectional leaky waves. Placing the feed in the middle of the antenna allows reducing the SLL, by keeping α (and β) constant along the whole antenna length. However, this method is only attractive for broadside radiation, since two mirrored beams are produced that eventually merge into a single beam having a maximum at broadside. This superposition of two beams that point always at different angles imposes an inherent limitation on the narrowest achievable beamwidth of bidirectional LWAs [9], [14], [15].

In this paper, a novel approach for designing a new type of untapered 1D LWA that produces a narrow main beam and low SLL is presented. In this technique, a right-handed (RH) and a left-handed (LH) propagating structures are combined with the aim of achieving a unidirectional leaky mode with a symmetrical amplitude pattern in the current distribution in a natural way. Moreover, with the introduced strategy, the

This work was supported by the Ministerio de Economia y Competitividad (MINECO)-Spain under Project PID2019-103904RB-I00. The authors are with the Departament d'Enginyeria Electrònica, Universitat Autònoma de Barcelona. 08193 BELLATERRA (Barcelona). Spain (e-mail: gerard.zamora@uab.es).

previously mentioned limitation on the narrowest achievable beamwidth of bidirectional LWAs is overcome.

A similar antenna arrangement as the one presented in this work was previously proposed for designing a zero beam-squinting LWA [16]-[18], and later for explaining the radiation from holographic surfaces [19]. In [16] and [17] two oppositely directed LWAs are designed with equal group delays and opposite phase velocities. In these works, the two employed transmission lines are parallel-connected. Such a parallel connection implies discontinuity of phase of the excited propagative mode at the intersection plane of the two branches. Thus, far-field radiation produced by the electric current flowing along the strip conductor of one branch is cancelled by the other branch in the direction where maximum radiation is expected. This effect can be appreciated in the radiation patterns shown in [17], where the cross-polar radiation exhibits a null at the direction where the main co-polar beam is maximum. However, in the demonstrating prototype presented in this work, continuity of phase of the propagating mode at the intersection plane of the two branches is achieved, so that there is no cancellation of the radiated fields. In [18] two LWAs are fed by a balun in the center in a similar way as in the antenna prototype presented in this paper. However, in contrast to the present work where off-broadside radiation is pursued, the two LWAs employed in [18] are both identical and have been designed to exhibit a phase constant $\beta = 0$ at the design frequency to achieve broadside radiation. In [19] it is mentioned that by using two branches with phase velocities equal in modulus but with opposite sign a unique beam with improved directivity (with respect to using only one branch) is obtained. However, the necessary condition of chosen the feed for guaranteeing continuity of phase (in addition of continuity of phase velocity) of the propagative mode in the intersection plane of the two sections is not disclosed. Moreover, in the present work the radiation characteristics of the proposed leaky-wave antenna configuration are analyzed and compared with experimental results for the first time.

II. Theory

A. Proposed Configuration

The proposed arrangement consists of a 1D left-handed (LH) open traveling-wave structure connected to a 1D right-handed (RH) open propagating structure, with absorbers at the ends (see Fig. 1). Both the LH and the RH sections are designed to propagate a fast wave with the phase constant equal in magnitude and of opposite sign. The feed is positioned at the intersection plane of the two sections and is chosen to ensure phase continuity of the propagative mode at said plane. Thus, a unidirectional leaky wave that travels from one end of the structure to the other with a double exponential amplitude distribution is produced along the antenna.

Leaky-wave antennas can be approximately modeled as a continuous line-source of electric current or magnetic current in the form of a wave traveling in free space [6]. Let us consider an electric current wave in free space traveling along the z-axis, with a double exponential amplitude distribution centered at $z = 0$, given by

$$I(z) = I_0 e^{-\alpha|z|} e^{-j\beta z} \tag{1}$$

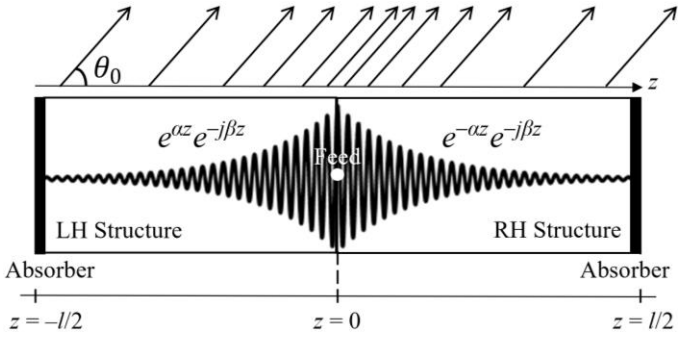

Fig. 1. Sketch of the proposed leaky-wave antenna configuration consisting of a left-handed fast-wave open guiding structure connected to a right-handed fast-wave open guiding structure, with a feed placed between them and absorbers at the ends. The current distribution that models the antenna and radiation emanating from the antenna are also illustrated.

where I_0 = constant. The time harmonic-dependence of the form $e^{j\omega t}$ is assumed throughout the paper. For simplicity, the leakage rate α was considered the same in both the LH and the RH sections, although in practical implementations they may differ from each other. Assume that the radiating current source has a finite length which extends from $z = -l/2$ to $z = +l/2$. The electric far-field radiated by such a current distribution may be described by considering only the θ-component (θ being the angle measured from the z-axis) and can be approximated by [13]

$$E_\theta(r,\theta) = j\eta_0 k_0 \frac{e^{-jk_0 r}}{4\pi r} \sin\theta \int_{-l/2}^{l/2} I(z) e^{jk_z z} dz \tag{2}$$

where η_0 and k_0 are, respectively, the characteristic impedance and wavenumber in free-space, and $k_z = k_0 \cos\theta$. The integral in (2) may be recognized as a Fourier transform type integral and is commonly designated as space factor (SF), which is analogous to the array factor for discrete-element antennas. Whereas the factor outside the integral is designated as element factor (or element pattern in arrays). The radiation intensity $U(\theta) = r^2|E_\theta|^2/2\eta_0$ due to the current distribution given in (1) is proportional to

$$U(\theta) \propto |\mathrm{SF}(\theta)|^2 \sin^2\theta \tag{3}$$

where the term $\sin^2\theta$ is the normalized radiation pattern for a z-directed current element [13]. It is worth mentioning that aperture-type LWAs are more appropriately modeled as a line-source distribution of magnetic current [6]. The space factor is then calculated by simply replacing $I(z)$ with the magnetic current into the integral in (2).

As it is known [13], for very narrow beam patterns, the total radiation intensity can be approximated by considering only the space factor (unless the element factor has a null at or in the vicinity of the direction of the main beam). With the help of (2), the magnitude square of the space factor due to (1) is found as

$$|\mathrm{SF}|^2 = \frac{4I_0^2 \left\{\alpha - e^{\frac{-\alpha l}{2}}\left[\alpha \cos\frac{kl}{2} - k \sin\frac{kl}{2}\right]\right\}^2}{\left(\alpha^2 + k^2\right)^2} \tag{4}$$

where $k = k_z - \beta$. As the length l of the radiating source tends to infinity, (4) reduces to

$$|\mathrm{SF}_\infty|^2 = \frac{4I_0^2\alpha^2}{\left(\alpha^2+k^2\right)^2} \tag{5}$$

Based on this simpler space factor, the angle of the main beam is determined as

$$\cos\theta_0 = \beta/k_0 \tag{6}$$

Equation (6) predicts that the radiation pattern will be in the form of a conical beam. The beamwidth for infinite length structures, evaluated when the maximum power is reduced by a factor of r, can also be calculated from (5) in a closed form. Considering a first order Taylor expansion of the term $\cos\theta$ around the angle of the maximum beam θ_0 (a valid approximation for narrow beams) we obtain

$$\Delta\theta_\infty = \frac{2\left(\sqrt{r}-1\right)^{\frac{1}{2}}(\alpha/k_0)}{\sin\theta_0} \tag{7}$$

B. Comparison with Single-Sided Leaky-Wave Antennas

Let us now consider a leaky-wave antenna operating in the usual way (i.e., with a feeding point at one end and an absorber at the opposite end), which can be approximately modeled by an electric current wave in free space

$$I^+(z) = I_0^+ e^{-\alpha z} e^{-j\beta z} u(z) \tag{8}$$

where I_0^+ = constant and u is the unit-step function. We chose the same length as in the previous structure (from $z = 0$ to $z = l$) by keeping the same phase constant β and leakage rate α as in (1), for comparison purposes. The space factor corresponding to (8) can be found in the literature (see for instance [6]) and its magnitude square may be expressed in the following alternative form:

$$|\mathrm{SF}^+|^2 = \frac{I_0^{+2}\left[1+e^{-2\alpha l}-2e^{-\alpha l}\cos kl\right]}{\alpha^2+k^2} \tag{9}$$

As it was demonstrated in [20], (6) is the exact formula for the angle of the beam maximum θ_0 predicted by (9).

Assuming an infinite length l of the structure, it is readily found that (9) reduces to

$$|\mathrm{SF}_\infty^+|^2 = \frac{I_0^{+2}}{\alpha^2+k^2} \tag{10}$$

From (10), it can be found the pattern beamwidth between the two points at which the power is reduced by a factor of r with respect to the maximum, for infinitely long structures, given by

$$\Delta\theta_\infty^+ = \frac{2\sqrt{r-1}(\alpha/k_0)}{\sin\theta_0} \tag{11}$$

Notice that (11) gives the well-known formula for the half-power beamwidth when $r = 2$ (see for instance [4]). It can be seen by comparing (7) with (11) that, for infinitely long antennas, a significant reduction of the beamwidth may also be achieved with the proposed method, given by

$$\frac{\Delta\theta_\infty^+}{\Delta\theta_\infty} = \left(\sqrt{r}+1\right)^{\frac{1}{2}} \tag{12}$$

In particular, the −3 dB beamwidth is reduced by a factor of 1.554, while the −10 dB beamwidth (calculated using $r = 10$) is lowered by a factor of 2. It is worth mentioning that (12) gives the maximum reduction factor for the beamwidth of practical LWAs, which corresponds to the limit when infinitely long structures are considered, as shown later.

Let us now compare the directivity, i.e., the maximum radiation intensity normalized to the radiation intensity averaged over all directions [13], with that of the previous LWA model. Assuming the same radiated power for both antennas, by equating the spatial integral of the magnitude square of (1) and (8), leads to

$$I_0^+ = I_0(1-\eta/2)^{\frac{-1}{2}} \tag{13}$$

where $\eta = 1-e^{-\alpha l}$ is the radiation efficiency (power radiated divided by power into the antenna) of the proposed antenna configuration. Notice that η differs from the usual expression for single-sided LWAs, namely $\eta^+ = 1-e^{-2\alpha l}$, and that $\eta < \eta^+$ for structures of finite length (for example, if $\eta = 90$ %, we have $\eta^+ = 99$ %). The ratio of the two directivities is then calculated as (4) over (9), both evaluated at the direction of the beam maximum (i.e., when $k = 0$), which leads to

$$\frac{D}{D^+} = \frac{2(2-\eta)\left(1-\sqrt{1-\eta}\right)^2}{\eta^2} \tag{14}$$

To validate the abovementioned analysis, we compare here the leaky-wave radiation predicted by the space factors due to the electric current (1) and (8), for finite and infinite-length structures. To this end, we consider $f_0 = 7$ GHz, $\alpha = 10$ nepers/m and $\beta = k_0/2 = 73.3$ rad/m which, from (6), leads to an angle of the main beam $\theta_0 = 60^\circ$. For the finite-length structures $l = 300$ mm was chosen so that $\eta = 95$ %, which in turn implies that $\eta^+ = 99.75$ %. It is interesting to show the normalized space factors due to (1) and (8) over the reciprocal space (see Fig. 2). As shown in Fig. 2, the space factors due to infinite-length structures exhibit a single lobe with the maximum located at $k_z = \beta$, as predicted by (6). Note that, the lobe due to (1) is narrower than the one related to (8), as predicted from (12). However, for finite-length structures the space factors exhibit a wider main lobe, and minor lobes emerge. This can be explained from the convolution theorem of the Fourier transform [21], which states that the convolution of two functions in one domain equals the product of the two functions in the transformed domain. Thus, SF (SF^+) can be seen as the convolution of SF_∞ (SF_∞^+) and the Fourier transform of a rectangular pulse of length l (i.e., the *sinc* function), defined from $z = -l/2$ to $z = +l/2$ ($z = 0$ to $z = l$). It is, therefore, expected that SF exhibits a narrower main lobe and lower minor lobes than SF^+ in the k-space, which leads to a narrower main beam and lower SLL in the far-field radiation pattern.

By examining (4) and (9) it was found that, given a specific value of the radiation efficiency, the same SLL was maintained for different values of the leakage rate.

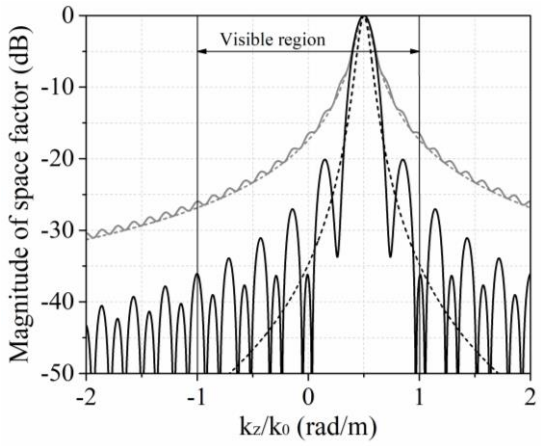

Fig. 2. Normalized space factor due to (1) in black lines and due to (8) in gray lines over the reciprocal space (*k*-space), considering infinite (dashed lines) and finite-length (solid lines) structures. The parameters are $f_0 = 7$ GHz, $\alpha = 10$ nepers/m, and $\beta = k_0/2$ rad/m. For the finite-length structures, it was considered $l = 300$ mm so that $\eta = 95$ %, which in turn implies that $\eta^+ = 99.75$ %. The indicated visible region is related to the physically observable angle θ.

Specifically, for $\alpha = 1$, 5 and 10 nepers/m the SLL due to (1) was found to be less than −20 dB for radiation efficiencies (η) in the range between 80 % and 100 % (i.e., practical efficiencies), as shown in Fig. 3. The −3 dB and −10 dB beamwidth reduction factors as a function of the radiation efficiency in the range between 80 % and 100 % were obtained from (4) and (9), by using the *Matlab* commercial software, and depicted in Fig. 4. It is worth mentioning that the same values (represented with symbols in Fig. 4) were obtained with different leakage rates, namely $\alpha = 1$, 5 and 10 nepers/m, suggesting that the beamwidth diminishing factor depends on the radiation efficiency rather than the leakage rate. Note that the −3 dB and −10 dB beamwidth increase factors are close to 1 for η lower than 95 % and 85 %, respectively. The reason is that for such values of η the beamwidth of both antennas is mainly determined by the beamwidth of the *sinc* function. Note also that the reduction factors shown in Fig. 4 approach the limit given by (12) as the radiation efficiency approaches 100 %. The directivity increase factor given by (14) was also depicted in Fig. 4. It shows a progressive growth from 0 dB as η becomes large, up to 3 dB in the limiting case of infinite antennas. Thus, the directivity of the proposed LWA will always be greater than that of the single-sided antenna for any value of $\eta > 0$, according to (14).

The normalized space factors obtained from (4), (5), (9) and (10) as a function of the angle theta are shown in Fig. 5. It can be verified that symmetric functions (with respect to $\theta = 0^o$) are obtained, according to a radiation pattern in the form of a conical beam with two main beams located at ±60º, as predicted by theory. It can be also seen that a significant reduction of the SLL can be achieved with the proposed technique. Although a similar −3 dB beamwidth is achieved for both antennas, the −10 dB beamwidth has been reduced by a factor of 1.65 according to the results shown in Fig. 4. Also, the directivity increase factor was found to be 1.403 (1.47 dB), according to (14).

In the strategy proposed in this work, the main beam is formed due to coherent radiation (i.e., same polarization and phase) of the two branches (RH and LH) in a particular

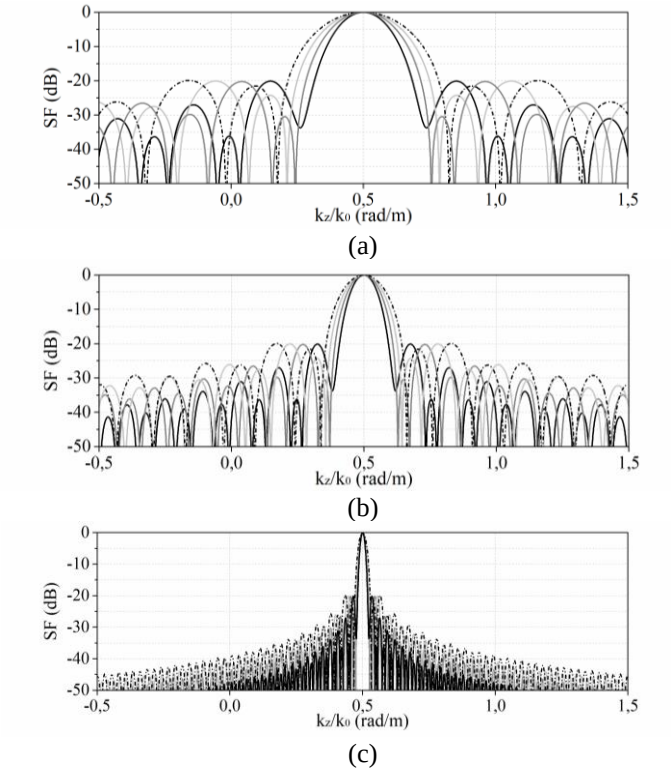

Fig. 3. Normalized space factor (4) over the reciprocal space (*k*-space) for $\eta = 95$ % (black solid lines), $\eta = 90$ % (dark gray solid lines), $\eta = 85$ % (light gray solid lines), and $\eta = 80$ % (black dash dot solid lines). The parameters are $f_0 = 7$ GHz, $\beta = k_0/2$ rad/m, and (a) $\alpha = 10$ nepers/m, (b) $\alpha = 5$ nepers/m, and (c) $\alpha = 1$ nepers/m.

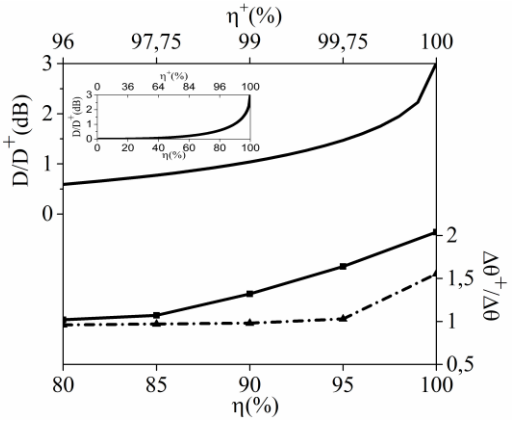

Fig. 4. Directivity increase factor (solid line) given by (14), and −3 dB (dot dashed line with symbol) and −10 dB (solid line with symbol) beamwidth reducing factor obtained from (4) and (9) as a function of the radiation efficiency of the proposed antenna η, and single-sided LWA η^+. A zoomed-out view of the directivity enhancement factor is also included. The parameters are $f_0 = 7$ GHz, $\beta = k_0/2$ rad/m, and $\alpha = 10$ nepers/m.

direction in space. Since the direction of maximum radiation from each of the branches varies with frequency in the reverse direction [16], there will be only a particular frequency at which the direction of maximum radiation from each of the branches coincide exactly, resulting in the radiation of a main beam with maximum gain and minimum width. Despite this, it is expected that the proposed structure keeps the radiation pattern fixed at such specific direction, allowing for the definition of a Zero Beam Squinting (ZBS) bandwidth. From the theoretical point of view, there is no limitation of achieving the same effect at any off-broadside angle from

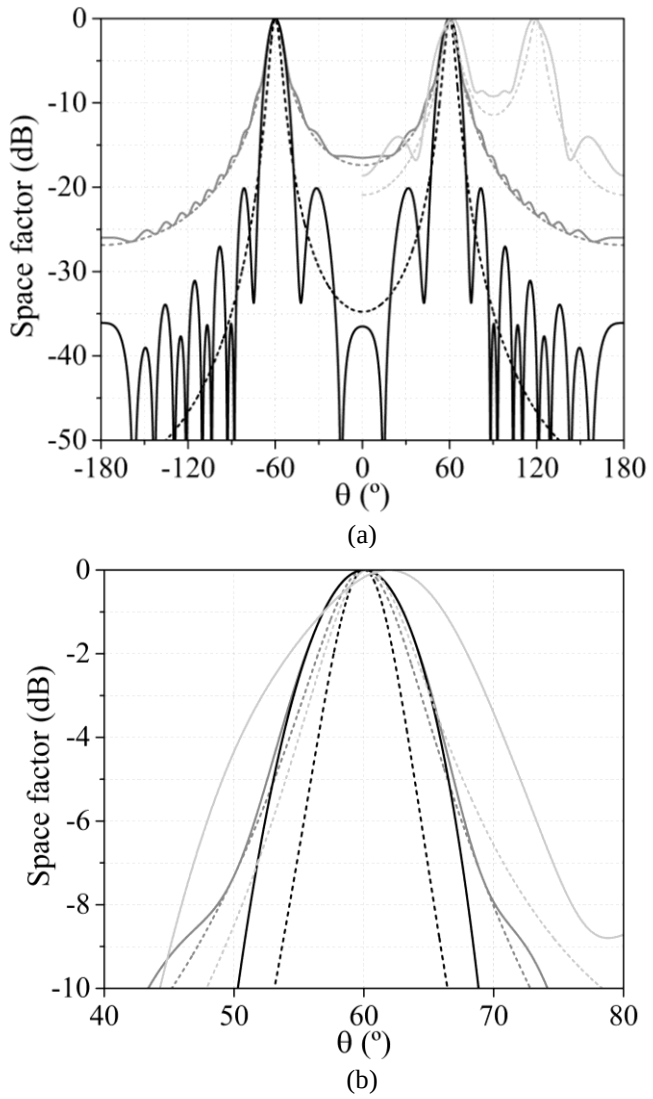

Fig. 5. (a) Normalized space factor due to (1) in black lines and due to (8) in dark gray lines, and normalized space factor due to (15) in light gray lines, considering infinite (dashed lines) and finite-length (solid lines) structures, and (b) zoomed-in view. The parameters are f_0 = 7 GHz, α = 10 nepers/m and $\beta = k_0/2$ rad/m. For the finite-length structures, it was considered l = 300 mm so that η = 95 %, which in turn implies that η+ = 99.75 %.

backfire to endfire. The only condition is that both the LH and RH arms of the LWA must have the capability of radiating at such specific angle.

C. Comparison with 1D Bidirectional Leaky-Wave Antennas

The beam properties of 1D bidirectional LWAs have been intensively investigated, with special emphasis in the case of broadside radiation (see, e.g., [14], [15], [22], [23]). It is well known that antennas supporting bidirectional leaky waves can produce a single broadside beam due to the coalescence of the two beams radiated from each symmetrical branch of the antenna, as mentioned in Section I. When operating at an off-broadside angle, a pair of conical beams, symmetrically positioned with respect to broadside, are produced. In contrast, the proposed structure generates a single conical beam at the designed frequency. Nevertheless, the radiation pattern produced by 1D bidirectional LWAs with a ground plane operating at an off-broadside angle is in the form of two half-conical beams symmetrical with respect to the broadside direction, which leads to two main beams in the longitudinal plane. It is therefore interesting to compare the radiation pattern from a bidirectional LWA having a ground plane with that of the LWA proposed in this work, which also has two main beams in the longitudinal plane.

Let us consider a 1D LWA that support a bidirectional leaky wave. The feed is placed in the middle of the structure (z = 0) and it is chosen to excite both halves of the structure symmetrically. The current distribution along the line source is now described by

$$I^B(z) = I_0 e^{-\alpha|z|} e^{-j\beta|z|} \tag{15}$$

In this case, the wave travels with identical phase velocities in both directions from the feed to the absorbing loads, placed at the ends of the structure ($z = \pm l/2$). It should be noted that the same current amplitude, I_0, as described in (1) has been considered. This ensures that the radiated power and radiation efficiency are identical to those of the proposed antenna. The magnitude square of the integral of (2) applied to (15) may be evaluated using (16), shown at the bottom of the page. For the case of an infinite length, (16) reduces to the following simpler form

$$\left|\mathrm{SF}_{\infty}^{\mathrm{B}}\right|^2 = \frac{4I_0^2\left(\alpha^2+\beta^2\right)}{\left(\alpha^2+k_z^2-\beta^2\right)^2+4\alpha^2\beta^2} \tag{17}$$

The normalized space factors derived from (16) and (17) as a function of the angle theta, specifically focusing on positive values of θ, are depicted in Fig. 5. This representation assumes the presence of a ground plane that effectively prevents radiation in directions where θ is negative. It can be appreciated two main lobes located near to 60º and 120º, respectively, symmetrically located about broadside. While the individual space factors of each branch would yield a single dominant beam directed at either 60° or 120°, according to (6), the combination of both radiation patterns results in a slight displacement (about 0.3° and 2° for the finite and infinite-length structures, respectively) of the resulting beams toward the broadside direction. As expected, the lobes generated by the infinite-length bidirectional LWA are narrower than for the finite-length structure.

In comparison to the proposed antenna, the bidirectional antenna exhibits a wider space factor under infinite length conditions. Consequently, the bidirectional LWA demonstrates a significantly larger beamwidth and higher SLL when compared to antennas of the same finite length. Specifically, the −3 dB beamwidth of the bidirectional antenna derived from (16) is 17.2° [see Fig. 5(b)], representing a 64% increase over the beamwidth (10.5°) of the proposed LWA. Additionally, the

$$\left|\mathrm{SF}^{\mathrm{B}}\right|^2 = 4I_0^2 \frac{\alpha^2+\beta^2+e^{-\alpha l}\left[\beta^2\cos^2\frac{k_z l}{2}+\left(\alpha\cos\frac{k_z l}{2}-k_z\sin\frac{k_z l}{2}\right)^2\right]-2e^{\frac{-\alpha l}{2}}\left[\left(\alpha^2+\beta^2\right)\cos\frac{\beta l}{2}\cos\frac{k_z l}{2}+k_z\left(\beta\sin\frac{\beta l}{2}-\alpha\cos\frac{\beta l}{2}\right)\sin\frac{k_z l}{2}\right]}{\left(\alpha^2+k_z^2-\beta^2\right)^2+4\alpha^2\beta^2} \tag{16}$$

SLL of the bidirectional LWA (−14 dB) is notably worse than the proposed antenna's (−20 dB). It is noteworthy that the derived half-power beamwidth value for the finite bidirectional antenna (17.2°) is in perfect agreement with the value obtained using the formula for the beamwidth of single-sided LWAs as presented in [20]. This concurrence arises from the fact that the half-power beamwidth of finite 1D bidirectional LWAs, operating at an off-broadside angle with $\beta >> \alpha$ (a condition considered satisfied for the case illustrated in Fig. 5, where β = 73.3 rad/m and α = 10 nepers/m), is equivalent to that for single-sided LWAs [23]. Therefore, under this condition, the half-power beamwidth of bidirectional antennas aligns with that of single-sided antennas with half the length, as they exhibit the same radiation efficiency. This accounts for the smaller half-power beamwidth of the single-sided LWA with a radiation efficiency of 99.75% compared to that of the bidirectional LWA of the same finite length, whose radiation efficiency is 95%, shown in Fig. 5.

The beam properties of 1D bidirectional LWAs were analyzed in [23]. We now summarize the evolution of the beam for the sake of completeness. Starting from the case of bidirectional structures with $\beta >> \alpha$ discussed in the previous paragraph, as β approaches α, the two lobes converge toward broadside, and the vicinity of the two peaks contributes to increasing the beamwidth of each lobe, unlike what occurs with single-sided LWAs. When β is slightly greater than the value corresponding to the splitting-point condition (i.e., $\beta = \alpha$ for infinite structures, and $\beta > \alpha$ for the finite-length case, in the latter β being a decreasing function of the radiation efficiency which tends to α as the radiation efficiency tends to infinity), the two symmetric beams merge to form an overall beam with two peaks close to broadside. Within this region (referred to as the scalloped region due to amplitude at broadside exceeds −3dB compared to the beam maximum level) the half-power beamwidth decreases as β decreases. Upon reaching the splitting-point condition, a broadside beam is obtained, whose beamwidth continuously decreases as $\beta < \alpha$, and it is minimized in the limit as β approaches 0.

In the specific case where $\beta = 0$, as proposed in [18], no bidirectional or unidirectional LWA exists, as there is no traveling wave. The beamwidth of infinite structures in the small beamwidth approximation is determined by equation (7) in this case, aligning precisely with the proposed antenna in the limit where the beam points in the broadside direction. In this limit, the half-power beamwidth for bidirectional antennas was calculated using Eq. 7 in [23], which is equivalent to (7) when r=2. However, this bandwidth-minimizing condition ($\beta = 0$) no longer holds when β and α are related, as in structures based on infinite-length scenario, the broadside beamwidth reaches a partially reflecting screens (PRS) excited by a bidirectional dipole-like source [14]. In such cases, specifically in the minimum at $\beta = 0.518\alpha$, resulting in a half-power beamwidth as specified by Eq. 7 in [23]. Compared to (7), the method proposed in this paper achieves a significant reduction in the half-power beamwidth under the limit where $\beta = 0$, with a reduction factor, in the narrow beams approximation, of $[(\sqrt{3}-1)(1+\sqrt{2})]1/2 \approx 1.329$.

It should be noted that the lobes generated by a bidirectional LWA with the lobes far from broadside (to minimize the interaction between the radiation generated by each branch) will exhibit approximately 3 dB lower directivity compared to what would be obtained by a single-sided LWA with half the length (i.e., a single branch of the bidirectional antenna) radiating the same power. In addition, the directivity of such a single-sided LWA would be, in turn, 3 dB lower than that of the proposed antenna under the same radiated power conditions, given that the aperture length in the latter is double. This leads to the expected directivity of the bidirectional antenna, in the absence of a ground plane, being approximately 6 dB lower than that of the antenna proposed in this work, and approximately 3 dB lower considering an ideal ground plane (capable of capturing all the back radiation). This analysis agrees with the obtained results, as the inferred directivity from (16), with an additional 3 dB to emulate the behavior of the bidirectional antenna in the presence of an ideal ground plane, was 2.7 dB lower than that of the proposed antenna.

For PRS-based 1-D bidirectional LWAs with infinite length, the directivity is maximized at broadside when $\beta = \alpha$. A comparison between (10) and (17) reveals that in the infinite-length case, bidirectional LWAs exhibit the same directivity at broadside as single-sided LWAs, and therefore, 3 dB lower than that of the proposed antenna in the limit where the beam points in the broadside direction.

III. Demonstrating Prototype

The designed leaky-wave structure is shown in Fig. 6. The antenna is essentially a 1D composite right/left-handed guiding structure consisting of a microstrip host line loaded with complementary split ring resonators (CSRRs), etched in the ground plane, and series gaps [24],[25]. Due to the loading, the fundamental quasi-TEM mode of the microstrip line turns into

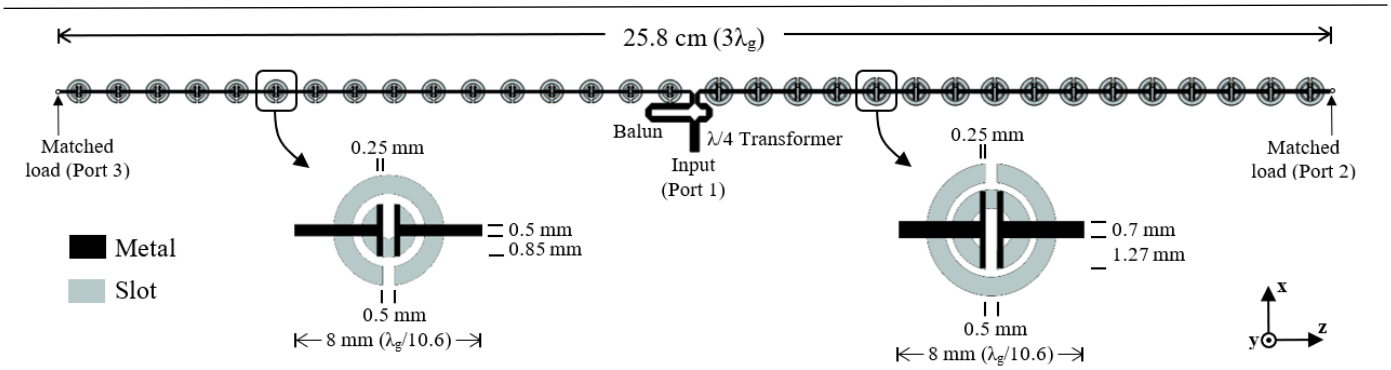

Fig. 6. Configuration of the proposed microstrip LWA and dimensions at 7.1 GHz. The external radius, ring width and ring separation of the CSRRs are respectively: i) 2.36 mm, 0.8 mm and 0.4 mm for the LH cell (left), and ii) 2.8 mm, 0.8 mm and 0.3 mm for the RH cell (right).

a fast wave and, therefore, radiation occurs from the fundamental $n = 0$ space harmonic. As shown in Fig. 6, the antenna has an asymmetrical configuration which basically consists of two different composite right/left-handed (CRLH) section lines terminated with matched loads at the ends. The left one was designed to propagate a fast backward wave with negative phase velocity. Whereas the right one was tailored to support a fast forward wave with phase velocity equal in magnitude and of opposite sign. Thus, at the operating frequency, a unidirectional leaky wave is propagated along the positive *z*-axis (see Fig. 6) with an exponentially increasing amplitude through the first half of the structure (LH section line) and exponentially decreasing along the second part (RH section line). The proposed antenna was designed to radiate the main beam pointing at $\theta_0 = 60°$ at an operating frequency of $f_0 = 7$ GHz, as a specific example. A *Rogers RO4003C* substrate with dielectric constant $\varepsilon_r = 3.42$, loss tangent $\tan\delta = 0.0027$ and thickness $h = 20$ mils was used. The period of the structure was fixed to $p = 8$ mm or, equivalently, $\lambda_g/10.7$ (λ_g being the guided wavelength at 7 GHz) to ensure that the homogeneity condition is well satisfied [5]. From (6), the required electrical length was found to be $\beta p = \pm 33.6°$ at 7 GHz, the upper (lower) sign standing for the RH (LH) unit cell. The Bloch impedance was set to 50 Ω at the operating frequency. The final dimensions of both the LH and the RH basic cells (see Fig. 6) were obtained with the help of the equivalent circuit model reported in [26]. The dispersion diagrams of the designed LH and RH elemental cells are depicted in Fig. 7, which were obtained from electromagnetic simulation (utilizing the *CST Microwave Studio* commercial software). It can be observed that the required electrical length for both unit cells is obtained at 7 GHz. The length of both the LH and RH section lines was chosen such that about 95 % of the input power is dissipated before reaching the 50 Ω antenna terminations. In order to ensure phase continuity of the propagative mode at the intersection plane, the two sections were connected in series by means of a balun, which was matched to the 50 Ω feed-line using a quarter-wavelength transformer. The balun design was inspired in the microstrip-to-cps transition proposed in [27]. The dimensions of the quarter-wavelength transformer and the balun are (see Fig. 8): $w_t = 1.75$ mm, $w_1 = 1.1$ mm, $w_2 = 0.75$ mm, $l_t = 6.1$ mm, $l_1 = 9.35$ mm, $l_2 = 2.4$ mm, $l_3 = 2.6$ mm, $l_4 = 3$ mm, $s = 0.25$ mm.

A photograph of both sides of the fabricated LWA prototype is shown at the top of Fig. 9. For comparison purposes, a single-sided LWA of the same length, based on the RH unit cell shown in Fig.6, was also fabricated (see Fig. 9 below). The measured *S*-parameters for both antennas are plotted in Fig. 10. For the two fabricated antennas, good impedance matching is observed at the operating frequency of 7 GHz. From the *S*-parameters of the single-sided antenna at the operating frequency ($S_{11} = -19$ dB and $S_{21} = -26$ dB) it was found that about 99.75 % of the power delivered to the antenna was dissipated before reaching the absorber. A straightforward calculation leads to a value for the attenuation constant $\alpha = 5.4$ nepers/m ($\alpha/k_0 = 0.062$). If we assume the same value of α for the proposed antenna, which applies strictly to the RH branch, it follows that 95 % of the power accepted by the antenna is dissipated before reaching the antenna terminations, as expected from theory.

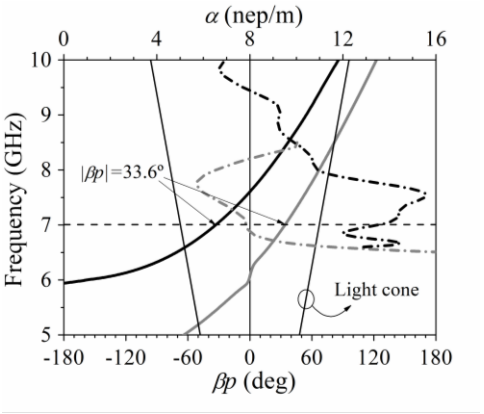

Fig. 7. Dispersion diagram of the designed left-handed (black lines) and right-handed (gray lines) unit cells including the phase constant (solid lines) and the attenuation constant (dot-dashed lines) obtained from electromagnetic simulation.

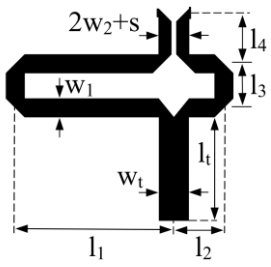

Fig. 8. Top view of the proposed balun and quarter-wavelength transformer.

The measured total gain normalized radiation patterns (i.e., the sum of the partial gains for any two orthogonal polarizations [13]) in the *yz*-plane of the two fabricated prototypes at the operating frequency are plotted in Fig. 11. Measurements were carried out in an anechoic chamber environment using a positioning system, a reference horn antenna (DE0518 broadband horn antenna) and an Agilent E8364B Programmable Network Analyzer. Notice that a bidirectional radiation pattern is obtained, as predicted by theory. As expected, the main radiation beam points at approximately $\theta_0 = 60º$. The SLL of the proposed LWA (−17 dB) is slightly higher than expected from theory (−20 dB), but significantly lower than that of the single-sided LWA (−10 dB). The small increase in the sidelobe levels of the proposed structure is attributed to parasitic radiation from the printed balun. The measured −3 dB beamwidth of the demonstrating prototype (11º) is in good agreement with the value (10.5º) obtained from the theoretical analysis. Although this experimental beamwidth is similar to that measured for the single-sided structure (12º), the −10 dB beamwidth (20º) has been reduced by a factor of 1.7 with respect to the single-sided LWA (34º), according to the analysis provided in Section II. The measured maximum total gain in the *yz*-plane of the proposed antenna and the one-sided LWA was found to be 12.8 dB and 11.2 dB, respectively, which corresponds to an increase factor of 1.44 (1.6 dB). This result is in good agreement with the value of 1.4 (1.5 dB) predicted by (14) for $\eta = 95$ %.

An additional measurement of the proposed antenna was made by including a ground plane in the bottom layer based on silver foil glued to a piece of expanded polystyrene with a thickness of 7 mm, i.e., less than a quarter of the wavelength

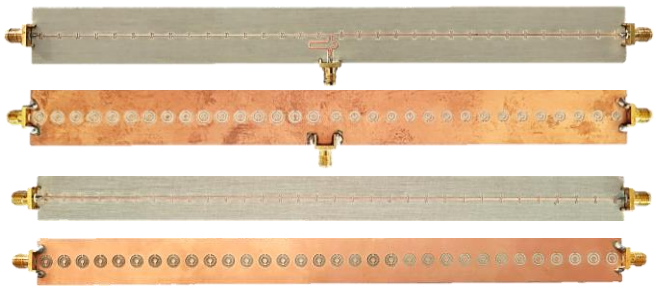

Fig. 9. Top and bottom views of the two fabricated CRLH leaky-wave antennas: (above) proposed antenna shown in Fig. 4 and (below) single-sided LWA of the same length.

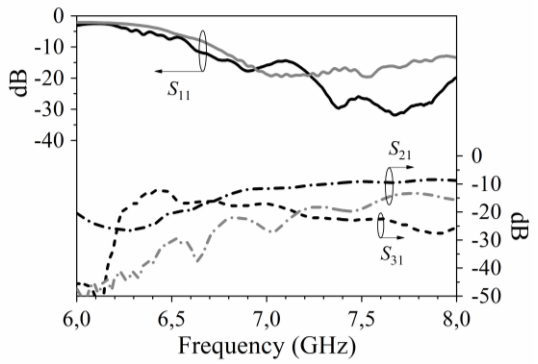

Fig. 10. Measured *S*-parameters of the proposed leaky-wave antenna (black curves) and the single-sided leaky-wave antenna (gray curves).

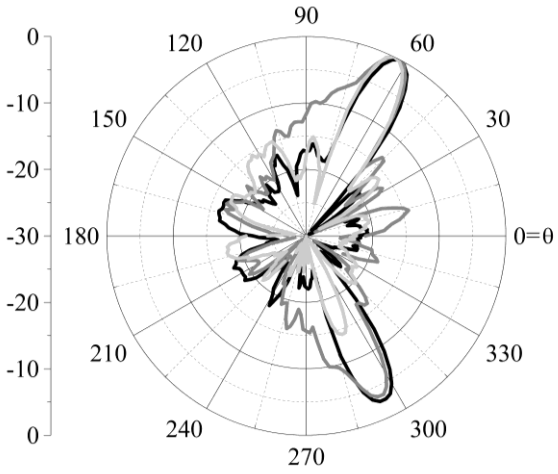

Fig. 11. Measured normalized total gain radiation pattern in the *yz*-plane of the proposed LWA (black line), the same antenna including a ground plane (light gray line), and the single-sided right-handed leaky-wave antenna (gray line), at the operating frequency.

(1.1 cm) at the operating frequency (7 GHz), to avoid excitation of a waveguide mode. The total normalized gain measured in the *yz*-plane is shown in Figure 11. Since an ideal and infinite ground plane was not utilized, the complete cancellation of radiation beneath the ground plane was not achieved. However, most of the radiation below the ground
plane has been attenuated to a level of approximately −15 dB with respect to the maximum gain. The radiation pattern above the ground plane closely resembles that of the antenna without a ground plane, with the main beam remaining almost identical. The measured maximum gain reached 14.4 dB, representing a 1.6 dB increase compared to the gain of the antenna without a ground plane. This indicates that a significant portion of the back radiation was successfully captured by the ground plane.

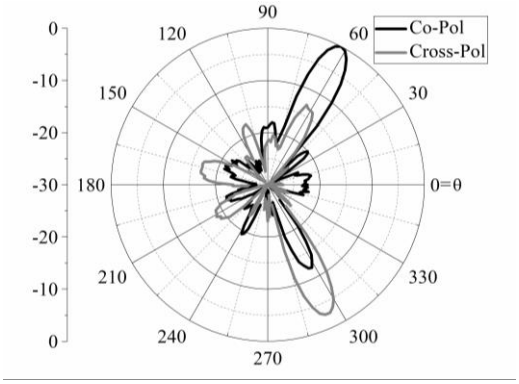

Fig. 12. Measured co-polarization and cross-polarization radiation patterns (*yz*-plane) of the proposed LWA normalized to the maximum value, at the operating frequency.

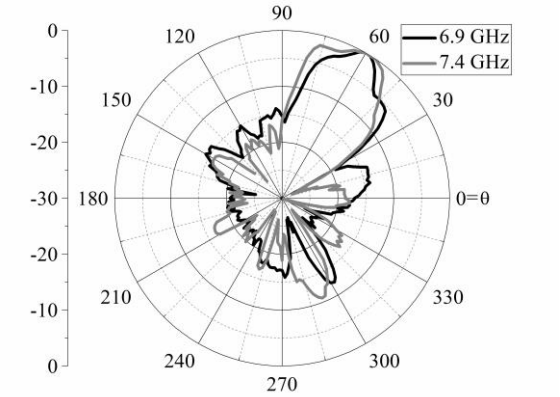

Fig. 13. Measured co-polarization normalized radiation patterns at the two edges of the ZBS bandwidth.

The measured co-polarization and cross-polarization radiation patterns of the proposed LWA are plotted in Fig. 12. Co-polarization radiation corresponds to right-handed circular polarization (RHCP) and cross-polarization to left-handed circular polarization (LHCP). It should be noted that LHCP dominates in the secondary beam of the total gain pattern shown in Fig. 11, whereas the main beam of the total gain can be considered predominantly right-hand circularly-polarized. The measured co-polar gain was found to be 12.6 dB.

The proposed antenna exhibits a fixed beam within the range of 7.4 GHz and 6.9 GHz, hence a ZBS bandwidth (defined as the frequency range for which the peak remains fixed at the direction of the maximum radiation) of 0.5 GHz or, equivalently, a relative bandwidth of 7 %. The radiation patterns at the two edges of the ZBS bandwidth are plotted in Fig. 13. At these frequencies, the co-polar gain at the direction of maximum radiation are 4.4 dB and 3.9 dB less than the maximum co-polar gain achieved at the operating frequency, respectively. At this point, the main beam is about to split into two [16].

IV. CONCLUSION

In this paper, a novel approach for designing LWAs with narrow main beam and low side lobe level is proposed. It consists in producing a unidirectional leaky wave with double exponential amplitude distribution along the antenna, which must be composed of a LH open structure and a RH open structure with a feed positioned between them and absorbers at the ends. A demonstrating prototype, based on a microstrip host

line loaded with CSRRs and series gaps is designed, fabricated and measured. A single-sided LWA operating in the usual fashion (i.e., with a feeding point at one end and a matched load at the opposite end) is also fabricated and measured, for comparison purposes. Good agreement between measured results with theory was observed. Moreover, A measurement of the proposed antenna with the presence of a ground plane has also been included. The results show that with the presented approach the beam of a single-sided LWA can be made significantly narrower, and the directivity may be simultaneously increased, compared to a conventional (single-sided) LWA with the same length, phase constant, and leakage rate. Moreover, a substantial reduction of the SLL may also be achieved by means of the presented design technique.

Additionally, a theoretical comparison with 1D bidirectional antennas operating at an off-broadside angle has been incorporated. The results indicate that the proposed strategy achieves a radiation pattern with a narrower beamwidth, smaller SLL and a directivity approximately 3dB higher than that of a 1D bidirectional antennas operating at an off-broadside angle and with a ground plane, which allows it to radiate under the same conditions as the proposed antenna, i.e., producing two main lobes in the longitudinal plane.

REFERENCES

[1] D. R. Jackson, C. Caloz and T. Itoh, "Leaky-Wave Antennas," *Proceedings of the IEEE*, vol. 100, no. 7, pp. 2194–2206, July 2012.

[2] F. Monticone and A. Alù, "Leaky-Wave Theory, Techniques, and Applications: From Microwaves to Visible Frequencies," *Proceedings of the IEEE* vol. 103, no. 5, pp. 793–821, May 2015.

[3] A. A. Oliner and D. R. Jackson, "*Leaky-wave antennas*," in *Antenna Engineering Handbook*, J. L. Volakis, Ed. New York, NY, USA: McGraw-Hill, 2007.

[4] D. R. Jackson and A. A. Oliner, "*Leaky-Wave Antennas*," in *Modern Antenna Handbook*, C. A. Balanis, Ed. New York: John Wiley & Sons, 2008.

[5] C. Caloz and T. Itoh, *Electromagnetic Metamaterials: Transmission Line Theory and Microwave Applications*, John Wiley & Sons, Hoboken, NJ, 2006.

[6] C. Caloz, D. R. Jackson, and T. Itoh, *"Leaky-wave antennas,"* in *Frontiers in Antennas: Next Generation Design & Engineering*, Frank B. Gross, Ed. New York: McGraw-Hill, Dec. 2011.

[7] A. A. Oliner, "Leaky waves: Basic properties and applications," in *Proc. Asia-Pacific Microw. Conf.*, vol. 1, pp. 397–400, Dec. 1997.

[8] M. García-Vigueras, J. L. Gómez-Tornero, R. Guzmán-Quirós, F. Quesada-Pereira, and A. Alvarez-Melcón, "Control of the radiation properties of a FSS loaded leaky-wave antenna," *Proceedings of the 4th European Conference on Antennas and Propagation (EuCAP)*, April, 2010.

[9] M. García-Vigueras, R. Guzmán-Quirós, and J. L. Gómez-Tornero, "Beamwidth control of 1D LWA radiating at broadside," *IEEE Proceedings of the 5th European Conference on Antennas and Propagation (EUCAP)*, April, 2011.

[10] M. García-Vigueras, P. DeLara-Guarch, J. L. Gómez-Tornero, R. Guzmán-Quirós, and G. Goussetis, "Efficiently illuminated broadside-directed 1D and 2D tapered Fabry-Perot leaky-wave antennas," *IEEE Proceedings of the 6th European Conference on Antennas and Propagation (EUCAP)*, March, 2012.

[11] R. Siragusa, E. Perret, P. Lemaitre-Auger, H. V. Nguyen, S. Tedjini and C. Caloz, "A Tapered CRLH Interdigital/Stub Leaky-Wave Antenna with Minimized Side-lobe Levels," *IEEE Antennas and Wireless Propag. Lett.*, vol. 11, pp. 1214–1217, Oct. 2012.

[12] Jeng-Hau Lu, Jie-Huang Huang, Christina F. Jou, and Lin-Kun Wu, "Side Lobe Suppression of a Short Leaky-Wave Antenna by Phase Constant Tapering: Analysis and Design," *IEEE Antennas and Wireless Propagation Letters, IEEE Trans. Antennas Propag.*, vol. 63, no. 8, pp. 3774–3779, June 2015.

[13] C. A. Balanis, *Antenna Theory: Analysis and Design*, 3rd Edition. New York, NY, USA: John Wiley & Sons, 2005.

[14] G. Lovat, P. Burghignoli, and D. R. Jackson, "Fundamental Properties and Optimization of Broadside Radiation From Uniform Leaky-Wave Antennas," *IEEE Trans. Antennas Propag.*, vol. 54, no. 5, pp. 1442–1452, May 2006.

[15] P. Burghignoli, G. Lovat, and D. R. Jackson, "Analysis and Optimization of Leaky-Wave Radiation at Broadside From a Class of 1-D Periodic Structures," *IEEE Trans. Antennas Propag.*, vol. 54, no. 9, pp. 2593–2604, Sep. 2006.

[16] K. M. Kossifos and M. A. Antoniades, "Analysis of an Off-Broadside Zero Beam-Squinting Leaky-Wave Antenna Using Metamaterials," *IEEE 18th Mediterranean Electrotechnical Conf. (MELECON)*, April 2016.

[17] K. Neophytou, K. Kossifos, and M. A. Antoniades, "An Off-Broadside Zero Beam-Squinting Leaky-Wave Antenna Based on NRI-TL Metamaterials", *IEEE Int. Symp. on Antennas and Propag. and North American Radio Science Meeting*, pp. 809-810, July 2020.

[18] K. Neophytou, K. Kossifos, and M. A. Antoniades, "A Circularly-Polarized Zero Beam-Squinting Leaky-Wave Antenna Using NRI-TL Metamaterials with Increased Gain," *Proceedings of the 15th European Conference on Antennas and Propagation (EuCAP)*, March, 2021.

[19] M. Nannetti, F. Caminita, and S. Maci, ''Leaky-wave based interpretation of the radiation from holographic surfaces,'' in *Proc. IEEE Antennas Propag. Int. Symp.*, pp. 5813–5816, June 2007.

[20] W. Fuscaldo, D. R. Jackson, and A. Galli, "A General and Accurate Formula for the Beamwidth of 1-D Leaky-Wave Antennas," *IEEE Trans. Antennas Propag.*, vol. 65, no. 4, pp. 1670–1679, Feb. 2017.

[21] R. N. Bracewell, *The Fourier Transform and its Applications*, 3rd Edition. New York: McGraw-Hill, 2000.

[22] A. Sutinjo, M., Okoniewski, and R. H. Johnston, "Beam-splitting condition in a broadside symmetric leaky-wave antenna of finite length," *IEEE Antennas and Wireless Propagation Letters*, vol. 7, pp. 609–612, July 2008.

[23] W. Fuscaldo, D. R. Jackson, and A. Galli, "General formulas for the beam properties of 1-D bidirectional leaky-wave antennas," *IEEE Trans. Antennas Propag.*, vol. 67, no. 6, pp. 3597–3608, March 2019.

[24] F. Falcone, T. Lopetegi, M. A. G. Laso, J. D. Baena, J. Bonache, M. Beruete, R. Marqués, F. Martín, and M. Sorolla, "Babinet Principle Applied to the Design of Metasurfaces and Metamaterials," *Physical Review Letters*, vol. 93, no. 19, pp. 197401, Nov. 2004.

[25] S. Eggermont and I. Huynen, "Leaky wave radiation phenomena in metamaterial transmission line based on complementary split ring resonators," *IEEE Microwave Opt. Tech. Lett.*, vol. 53, no. 9, Sept. 2011.

[26] J. Bonache, M. Gil, O. García-Abad, and F. Martín, "Parametric Analysis of Microstrip Lines Loaded with Complementary Split Ring Resonators," *Microwave and Optical Technology* Letters, vol. 50, no. 8, August 2008.

[27] Y. Qian and T. Itoh, "A Broadband Uniplanar Microstrip-to-CPS Transition," *Proceedings of 1997 Asia-Pacific Microwave Conference*, Dec. 1997.

Gerard Zamora Gonzalez (M'14) was born in 1984 in Barcelona (Spain). He received the Telecommunications Engineering Diploma, specializing in Electronics from the Universitat Autònoma de Barcelona in 2005. He obtained the Telecommunications Engineering degree in 2008 and the PhD degree in Electronics Engineering from the same university in 2013. His current research interests include active and passive microwave devices, metamaterials, antennas and RFID.

Jordi Bonache (S'05–M'07) was born in Cardona (Barcelona), Spain, in 1976. He received the Physics and Electronics Engineering degrees and the Ph.D. in electronics engineering from the Universitat Autònoma de Barcelona, in 1999, 2001 and 2007, respectively. In 2000, he joined the High Energy Physics Institute of Barcelona, where he was involved in the design and implementation of the control and monitoring system of the MAGIC telescope. In 2001, he joined the Department of Electronics Engineering, Universitat Autònoma de Barcelona, where he is currently Professor of Electronics. From 2006 to 2009, he was the Executive Manager of CIMITEC, Bellaterra, Spain. His current research interests include active and passive microwave devices, metamaterials, antennas and RFID.